

A bond graph approach to energy efficiency analysis of a self-powered wireless pressure sensor

Yong Cui[†], Robert X. Gao[‡] and Dengfeng Yang[†]

Department of Mechanical and Industrial Engineering, University of Massachusetts, Amherst, MA 01003, USA

David O. Kazmer^{‡†}

Department of Plastics Engineering, University of Massachusetts, Lowell, MA 01854, USA

(Received July 29, 2004, Revised March 28, 2006, Accepted April 13, 2006)

Abstract. The energy efficiency of a self-powered wireless sensing system for pressure monitoring in injection molding is analyzed using Bond graph models. The sensing system, located within the mold cavity, consists of an energy converter, an energy modulator, and a ultrasonic signal transmitter. Pressure variation in the mold cavity is extracted by the energy converter and transmitted through the mold steel to a signal receiver located outside of the mold, in the form of ultrasound pulse trains. Through Bond graph models, the energy efficiency of the sensing system is characterized as a function of the configuration of a piezoceramic stack within the energy converter, the pulsing cycle of the energy modulator, and the thicknesses of the various layers that make up the ultrasonic signal transmitter. The obtained energy models are subsequently utilized to identify the minimum level of signal intensity required to ensure successful detection of the ultrasound pulse trains by the signal receiver. The Bond graph models established have shown to be useful in optimizing the design of the various constituent components within the sensing system to achieve high energy conversion efficiency under a compact size, which are critical to successful embedment within the mold structure.

Keywords: Bond graph modeling; self-powered sensing; energy efficiency of sensors; condition monitoring of manufacturing process.

1. Introduction

With the prolific use of sensors for mechanical system and civil structure condition monitoring and the growing demand for system integration, the issue of sensor powering has assumed an increasingly central role. Powering through cable connections, while commonly seen on the factory floor, face constraints in field applications. Battery-based operation, although compact and eliminating the cable attachment, has the ultimate drawback of requiring periodic replacement due to wear-and-tear. Thus, extracting energy from the system or structure being monitored itself becomes a logical solution (Gao, *et al.* 2002, Theurer, *et al.* 2003). The deployment of a self-powered sensor is particularly attractive for

[†]Graduate Student

[‡]Professor, Corresponding Author, E-mail: gao@ecs.umass.edu

^{‡†}Professor, E-mail: david_kazmer@uml.edu

monitoring the injection molding process, given the high temperature, high pressure nature of the process, and the various practical constraints in process measurement from within an enclosed, metallic environment.

Direct measurement of cavity pressure and temperature has shown to provide a better indicator for the final part quality produced by the injection molding process than by any indirect methods (Rawabdeh and Petersen 1999, Watkins 1997). Wired pressure sensors, while still commonly used on the factory floor, face various constraints. Because of the structural complexity of most injection molds, the cost to modify the mold in order to install a wired sensor can be significant. A self-powered wireless pressure sensor was developed (Theurer, *et al.* 2003) that provides a direct cavity pressure measurement for the injection molding process. In this approach, an acoustic wave, instead of an electromagnetic wave, was used as the information carrier to overcome transmission shielding problems due to the mold steel surrounding the transmitter. Measurement of the mold cavity pressure was achieved by using a series of ultrasonic pulses generated when the change in pressure exceeded a preset threshold value. By summing up the number of pulses received, the overall pressure applied to the sensor could be retrieved. The energy extraction was realized by the piezoceramic energy converter, which converts the mechanical pressure of the polymer melt into proportional electrical charges. The energy extracted in each pulsing cycle determines the magnitude of the ultrasound signal that is subsequently sent through the injection mold by the transmitter. This implies that the accuracy of the reconstructed mold cavity pressure is affected by the sensitivity of the receiver outside the mold.

Given the intrinsic limitations of such a self-powered sensing technique, it is important to analyze the energy efficiency of each constituent components of the sensor system in order to fully utilize the limited amount of energy extracted from the polymer melt to achieve optimal sensing result. The energy efficiency of each component can be obtained by the ratio of the output and input energy associated with the component, which in turn can be calculated using a generalized model that takes into account the dynamic behavior of the sensing system within each injection pulsing cycle. However, given the multi-domain (e.g. mechanical, electrical, thermal) nature of the sensing system and its structural complexity, it is difficult to derive an overall system model by using conventional block diagram or circuit modeling techniques (Theurer, *et al.* 2003, Zhang, *et al.* 2003) to simultaneously cover parameters in various domains. The Bond graph approach, in comparison, provides a uniform mechanism for the description of systems with a multiplicity of physical domains (Karnopp and Rosenberg 1968). There are several advantages in using the Bond graph technique for complex system modeling. First, the Bond graph uses a relative small number of symbols and elements to represent a system that generally would need a large number of differential equations to be adequately represented (Karnopp, *et al.* 2000). Second, the Bond graph models developed can be processed in a standard procedure to produce block diagrams or first-order differential equations for easy post-processing, making it possible to quantitatively determine specific variables in conjunction with commercial software packages such as MATLAB (Montgomery and Granda 2003). Third, given proper causality considerations, the Bond graph models can be handled in a “plug-and-play” manner (McBride and Cellier 2003), thus providing flexibility in the modeling process. Finally, Bond graph models of systems with complex dynamics can be used directly for system simulation, thus providing direct input to improving system design (Youcef-Toumi 1996).

Extensive research has been conducted using Bond graph for modeling cross-domain systems. In Margolis and Shim (2001), the Bond graph representation of a four-wheel, nonlinear vehicle dynamic model with electrically controlled brakes and steering was developed. The efficiency of a hydraulic system was analyzed based on the Bond graph model (Sakurai 2000). However, there have been relatively few reported studies on modeling piezoelectric energy generators using Bond graph models. In

Goldfarb and Jones (1999), the Bond graph model of a piezoceramic power generator was developed to describe the dynamic coupling between mechanical and electrical domains. The efficiency of the system was analyzed in terms of the frequency of input force. A similar Bond graph approach was used in their previous work (Goldfarb and Celanovic 1997), for modeling a piezoelectric actuator. In these works, transformers (TF) were employed to establish the energy transfer between mechanical and electrical domains. However, the issue of determining transformer modulus was not addressed. In Busch-Vishniac and Paynter (1991), Bond graph models of acoustical transducers were proposed to overcome limitations of the traditional pure circuit model approach that lacks sound connection to the physical world.

This paper introduces a Bond graph approach to analyzing the energy efficiency of a wireless pressure sensing system for on-line pressure sensing from within the injection mold cavity. Bond graph models of various components in the sensing environment are first developed, assuming an isothermal environment within the sensor package. Based on these models, a unified energy efficiency model of the entire sensing system is established. Subsequently, relationship between the input and output variables are established to analyze the energy efficiency of the sensing system. The obtained energy model is then used to identify the minimum level of signal intensity required to ensure successful detection of the signal by the receiver outside of the injection mold. Finally, the developed energy efficiency model is verified by two experimental case studies. A systematic and detailed demonstration of the Bond graph technique to modeling and analyzing the energy efficiency of a complex, self-powered wireless pressure sensing system is the main contribution of this paper, whereas the modeling results can be used for future improvement of the sensor packaging design.

2. Sensing principle

As illustrated in Fig. 1, the pressure sensor consists of four major components located within the injection mold (i.e. a top insulator, an energy converter, a threshold modulator, which functions as an electronic switch, and an ultrasonic signal transmitter) and a signal receiver located outside of the mold cavity. The insulator presents a thermal barrier to prevent the polymer melt of high temperature from heating up the sensor components, thus providing a near isothermal environment within the sensor

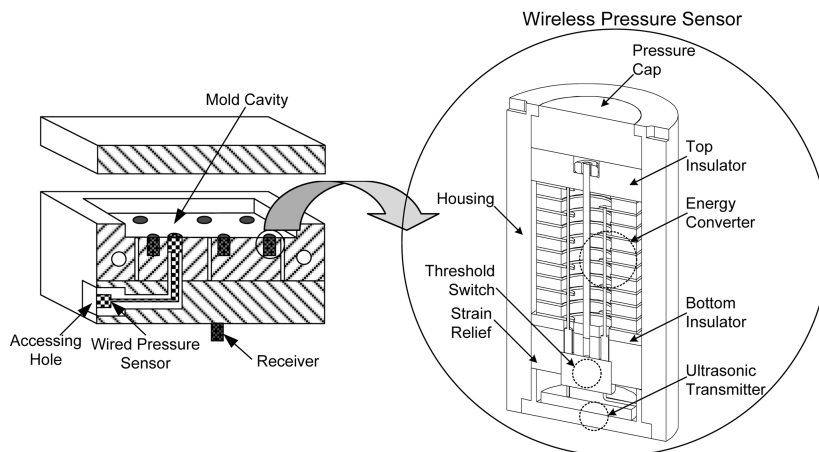


Fig. 1 Illustration of self-powered wireless pressure sensors installed within the mold cavity

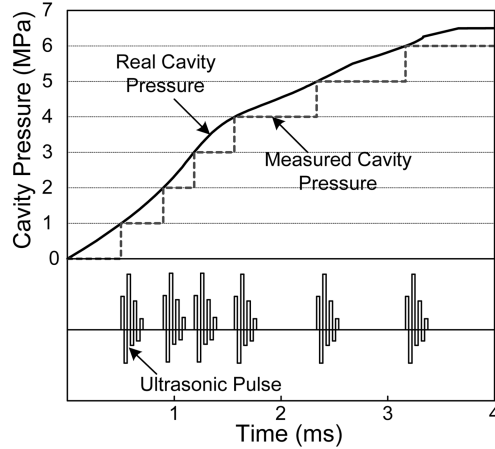


Fig. 2 Digitization of the mold cavity pressure through ultrasonic pulse trains

(Theurer, *et al.* 2003). The energy converter is made of a stack of concentric piezoceramic rings, which develops an electrical charge proportional to the polymer melt pressure exerted on the stack. The developed charge is stored in a parallel capacitor in the form of a voltage, which provides a direct measure for the mechanical pressure. Each time the voltage across the capacitor exceeds a preset threshold level, the threshold modulator will release the accumulated charge to the signal transmitter in the form of an electrical pulse. Upon such an impulsive excitation, the signal transmitter generates a train of ultrasonic pulses that propagates through the mold steel to the signal receiver (Zhang, *et al.* 2003).

After each such pulsing cycle, the collected charge will be released and the modulator deactivated, resetting the system for the next cycle. As a result of such a repetitive process, the cavity pressure is discretized by a series of ultrasonic pulse trains. The actual cavity pressure profile can be then reconstructed by multiplying the total number of the pulse trains with the preset pressure threshold values. In Fig. 2, the solid curve represents the actual pressure exerted by the polymer melt on the mold cavity, and the dashed curve is the reconstructed pressure from the ultrasound pulses, which is generated each time when the cavity pressure exceeds a preset pressure threshold value. Thus, the threshold setting directly affects the energy efficiency of the sensing system, since the continuous pressure curve is represented by the number of discrete ultrasonic pulse trains. To quantitatively determine the energy efficiency of the sensing system, a cross-domain modeling approach is taken, as described below.

3. System model formulation

To analyze the energy efficiency of the sensing system, Bond graph models for the constituent components are first constructed, based on the relationship between the input and output variables in the respective domains, e.g., *force* and *velocity* in the mechanical domain, and *voltage* and *current* in the electrical domain. As illustrated in Fig. 3, the energy modulator functions as an electrical switch to control the energy flow from the energy converter to the ultrasonic signal transmitter. When the output voltage of the energy converter drops below a preset threshold value, the modulator will be turned *off*. Conversely, when the voltage exceeds the preset threshold, the modulator will turn the circuit *on*, relaying an electrical current pulse to the ultrasonic transmitter, which in turn transmits a train of

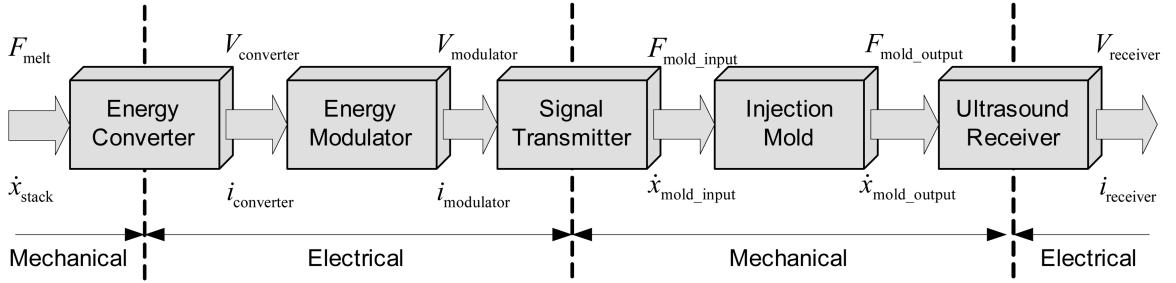


Fig. 3 Energy flow across various domains along the sensor and injection mold

ultrasonic pulses through the injection mold steel to the receiver. Given this functionality, the modulator is modeled as a resistor with infinite resistance in its *off* state and zero resistance in the *on* state. Prior study (Theurer, *et al.* 2003) has verified that the energy loss of the modulator is less than 0.7% of the total input energy. Thus it is considered negligible and not included in the present Bond graph model.

3.1. Model of the energy converter

The energy converter consists of a stack of concentric rings made out of piezoceramic materials (PZT). The stack produces an electrical charge proportional to the mechanical stress applied to it. To achieve high ultrasound signal strength for high signal-to-noise sensing, the 33 mode¹ of the piezoceramic is utilized. Given the relatively slow pressure application from the polymer melt (1~2 seconds per molding or pulsing cycle), the effect of shock wave is ignored, and the piezoceramic stack is mechanically represented by a mass-spring-damper system, as shown in Fig. 4. During each pulsing cycle, the melt pressure applied to the stack is modeled as a ramp input. The parameters m_{stack} , b_{stack} , and k_{stack} represent the mass, damping, and stiffness constants of the stack under the longitudinal mode of vibration (Goldfarb and Jones 1999), and n_{ir} is the electromechanical transformer modulus, which describes the energy transferred from the mechanical domain to the electrical domain. The symbols C_{stack} and $C_{parallel}$ represent the capacitance of the piezoceramic stack and an external parallel capacitor, respectively, and R_m represents the resistance of the threshold modulator. The purpose of adding a parallel capacitor is to attenuate the high output voltage from the stack (on the order of 100~1,000 V) down to within 1~10 V for ease of handling.

The Bond graph of the energy converter was constructed based on the relationship between the energy input port (with the melt force expressed as $F = PA$, where P is the melt pressure, and A is the surface area of the pressure cap) and voltage output port (V_{ir}). As shown in Fig. 5, the energy conversion process was modeled as a *transformer* (TF), with the left portion of the transformer describing the mechanical domain, and the right portion describing the electrical domain. In the mechanical domain, the melt force represents the *effort* and the stack velocity (time derivative of the stack displacement under melt force) is the *flow*. Correspondingly in the electrical domain, the electrical voltage V_{ir} represents the *effort* and the current i represents the *flow*. The product of these signal pairs in the Bond graph represents the power of the system. The effect of damping in the mechanical part is described as a

¹The 33 mode implies that charges are collected on the electrode surface perpendicular to the polarization direction when tensile or compressive mechanical forces are applied along the polarization axis.

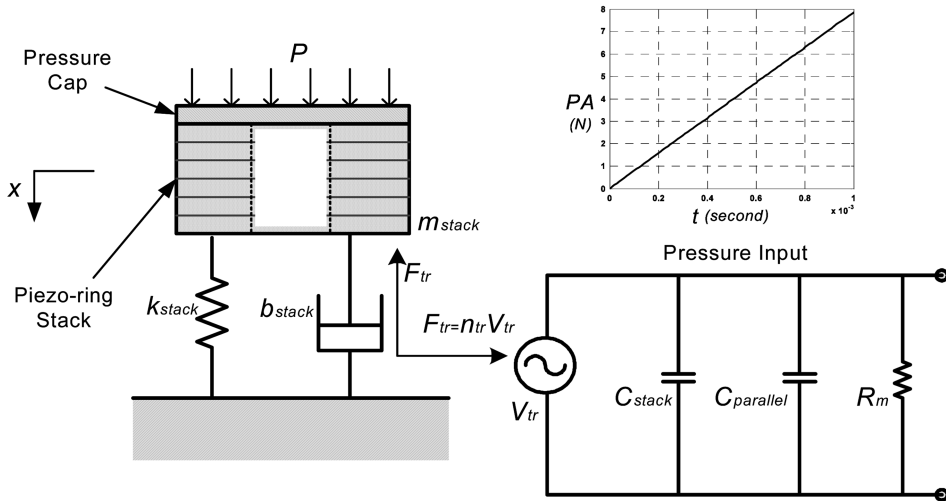


Fig. 4 Schematic representation of the piezoceramic energy converter

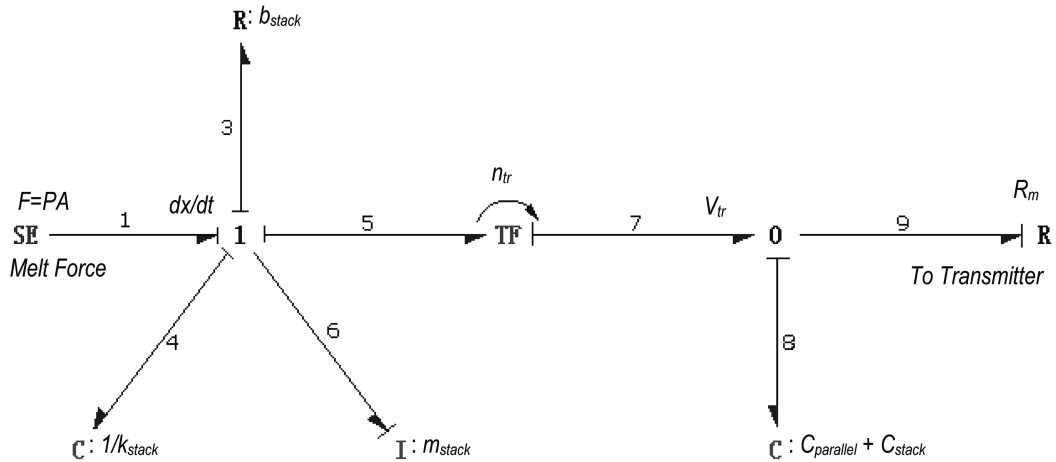


Fig. 5 Bond graph representation of the energy converter

resistance element, the stack stiffness as a capacitance element, and the mass as an inertia element. The energy flow to the R , C and I components accounts for the energy loss during the mechanical-electrical energy conversion. The energy Bond 5 represents the energy flow from the mechanical domain to the electrical domain. The effort junction (1 junction) on the mechanical side illustrates that the stack has the same flow (velocity) but different effort (force), while the flow junction (0 junction) on the electrical side illustrates that the circuit has the same effort (voltage) but different flow (current).

According to the laws of energy conservation and causality, following relationship can be established:

$$F_{tr} \dot{x} = V_{tr} i \quad (1)$$

$$F_{tr} = n_{tr} V_{tr} \quad (2)$$

$$q = n_{tr} x_{stack} \quad (3)$$

where F_{tr} is the transduced force in the mechanical domain, V_{tr} is the voltage across the stack, q is the total charge in the electrical domain, and x_{stack} is the stack displacement under the melt pressure. From Eq. (1), the power developed in the mechanical domain is transferred to the electrical domain, with the transformer modulus n_{tr} given by (refer to *Appendix A* for derivation):

$$n_{tr} = \frac{nAd_{33}Y}{h} \quad (4)$$

In Eq. (4), Y is the Young's modulus of the piezoceramic material, d_{33} is the piezoelectric charge constant, n is the number of piezoceramic rings in the energy converter stack, and h is the thickness of the rings. As shown in Eq. (4), thinner piezoceramic rings (smaller h) lead to larger n_{tr} . This in turn reduces the output voltage V_{tr} delivered by the stack, for a given F_{tr} (transduced force at the end of a pulsing cycle), as per Eq. (2). Such a voltage reduction mechanism inherent to the energy converter design can be utilized to minimize the external parallel capacitor, so that the output voltage can be kept within an easy-to-handle range while maintaining the efficiency of the energy conversion process.

The mechanical energy exerted on the energy converter by the polymer melt in each pulsing cycle was calculated as:

$$W_{mech} = \int_0^{t_p} P(t) A x_{stack}(t) dt \quad (5)$$

The total electrical energy available at the electrical side of the energy converter is:

$$W_{elec} = \frac{1}{2} (C_{stack} + C_{parallel}) V_{tr}^2 \quad (6)$$

where V_{tr} is the output voltage of the threshold modulator (refer to *Appendix B* for details). Consequently, the energy efficiency of the energy converter is given by:

$$\eta_{converter} = \frac{W_{elec}}{W_{mech}} \quad (7)$$

3.2. Model of the signal transmitter

The ultrasonic signal transmitter (shown in Fig. 6) is approximately 10 mm in diameter and consists of a multi-layered assembly: a piezoelectric layer (0.6~1.5 mm) that vibrates along its axial direction upon electrical excitations, a front layer (0.3~1.5 mm) that couples to the injection mold steel, and a bonding layer (50~60 μm) that connects the piezoelectric and front layers (Zhang, *et al.* 2005). Due to the large aspect ratio of the transmitter (diameter/thickness >10), the thickness extensional mode vibration is dominant over other modes. In order to analyze the energy efficiency of the transmitter, the relationship between the output *force* and *velocity* at the front layer and the input *force* and *velocity* at the piezoelectric layer needs to be determined. Instead of solving the wave equations directly, the equivalent circuit modeling approach (Zhang, *et al.* 2003) (Sittig 1969) was employed to simplify the solution procedure.

The Bond graph model of the piezoelectric layer of the transmitter is shown in Fig. 7, with the energy

where ε is the permittivity. The transformer modulus m_{tr} is expressed as:

$$m_{tr}^2 = \omega_0 C_0 Z_0 k^2 / \pi \quad (12)$$

where k is the electromechanical coupling factor. Based on the Bond graph model, the relationship between the input voltage V_{tr} and current I_{tr} and the output force F_t and velocity u_t were obtained as:

$$\begin{bmatrix} V_{tr} \\ I_{tr} \end{bmatrix} = \begin{bmatrix} A_0 & B_0 \\ C_0 & D_0 \end{bmatrix} \begin{bmatrix} F_r \\ u_t \end{bmatrix} \quad (13)$$

The transformation matrix in Eq. (13) can be further expressed as:

$$\begin{bmatrix} A_0 & B_0 \\ C_0 & D_0 \end{bmatrix} = \frac{1}{m_{tr} Q} \begin{bmatrix} 1 & jm_t^2 / (\omega C_0) \\ j\omega C_0 & 0 \end{bmatrix} \begin{bmatrix} \cos \gamma_0 + jz_b \sin \gamma_0 & Z_0(z_b \cos \gamma_0 + j \sin \gamma_0) \\ (j \sin \gamma_0) / Z_0 & 2(\cos \gamma_0 - 1) + jz_b \sin \gamma_0 \end{bmatrix} \quad (14)$$

where $Q = \cos \gamma - 1 + jz_b \sin \gamma$ and $z_b = Z_b / Z_0$. The parameter Z_b represents the impedance of the back face of the piezoelectric layer, which is zero due to the air backing design in the present system.

The front layer is expressed in the Bond graph as shown in Fig. 8, where F_t and u_t are the input force and velocity from the piezoelectric layer, and F_f and u_f are the output force and velocity to the mold.

The relationship between the input and output is given as:

$$\begin{bmatrix} F_t \\ u_t \end{bmatrix} = \begin{bmatrix} A_1 & B_1 \\ C_1 & D_1 \end{bmatrix} \begin{bmatrix} F_f \\ u_f \end{bmatrix} \quad (15)$$

where the transformation matrix is given as:

$$\begin{bmatrix} A_1 & B_1 \\ C_1 & D_1 \end{bmatrix} = \begin{bmatrix} \cos \gamma_1 & jZ_1 \sin \gamma_1 \\ (j \sin \gamma_1) / Z_1 & \cos \gamma_1 \end{bmatrix} \quad (16)$$

In Eq. (16), the symbols Z_1 and γ_1 represent the mechanical impedance and normalized frequency of the

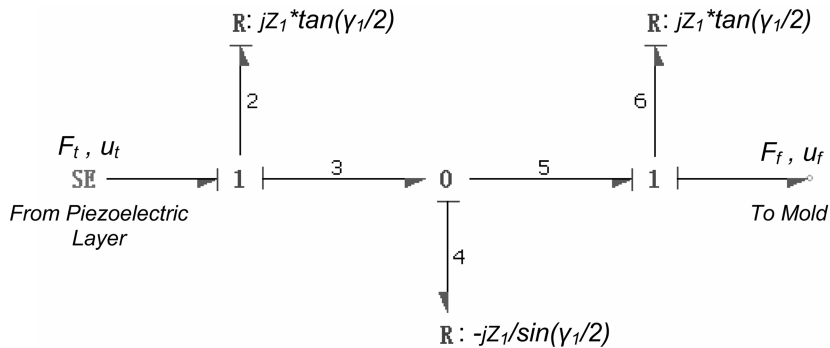


Fig. 8 Bond graph model of the front layer

front layer, respectively. They were determined by following the same approach as illustrated in modeling the piezoelectric layer. The input-output relationship for the entire transmitter can be obtained by combining the models for the piezoelectric layer and front layers together. Specifically, multiplying the matrices for the two layers, the overall matrix that relates the excitation voltage V_{tr} and current I_{tr} to the piezoelectric layer to the sound force F_f and velocity u_f (output to the mold steel) can be obtained as:

$$\begin{bmatrix} A_t & B_t \\ C_t & D_t \end{bmatrix} = \begin{bmatrix} A_0 & B_0 \\ C_0 & D_0 \end{bmatrix} \times \begin{bmatrix} A_1 & B_1 \\ C_1 & D_1 \end{bmatrix} \quad (17)$$

and

$$\begin{bmatrix} V_{tr} \\ I_{tr} \end{bmatrix} = \begin{bmatrix} A_t & B_t \\ C_t & D_t \end{bmatrix} \begin{bmatrix} F_f \\ u_f \end{bmatrix} \quad (18)$$

Consequently, the transfer function relating the input voltage V_{tr} to the output sound force F_f is derived as:

$$V_{tr} = \frac{A_t Z_{0t} + B_t + Z_s (C_t Z_{0t} + D_t)}{Z_{0t}} F_f \quad (19)$$

where Z_{0t} is the mechanical impedance of the mold steel, and $Z_s = R_s + jX_s$ represents the electrical impedance of the signal generation source (i.e. the threshold modulator within the pressure sensor) that excites the transmitter. Consequently, the energy efficiency of the energy transmitter through the steel mold is expressed as:

$$\eta_{transmitter} = \frac{P_{output}}{P_{input}} = \frac{F_f u_f}{V_{tr} I_{tr}} = \frac{Z_{0t}}{[A_t Z_{0t} + B_t + Z_s (C_t Z_{0t} + D_t)][C_t Z_{0t} + D_t]} \quad (20)$$

3.3. Model of the injection mold and receiver

Ultrasound waves dissipate energy when traveling through a medium due to wave scattering and absorption. The energy attenuation at a given frequency can be expressed as:

$$F_r = F_f e^{-\frac{\alpha h_m}{20}} \quad (21)$$

where F_r is the output *force* from the ultrasonic transmitter to the receiver. The symbol h_m represents the thickness of the mold, and α is the attenuation coefficient, which is $\alpha = 110$ dB/m for a longitudinal ultrasonic pulse of 2 MHz traveling through a steel block (Bray and McBride 1992). For a 40 mm steel mold, the output *force* can be attenuated to 80% of the input *force*.

For purpose of simplicity, the receiver was modeled in a reversed process as that of the transmitter. Therefore, the energy transformation modulus m_{re} of the receiver from the mechanical domain to the electrical domain is the reciprocal of the transformation modulus m_{tr} from the electrical domain to the mechanical domain. Similarly, the governing matrices for the receiver (A_r , B_r , C_r , and D_r) were derived using Eqs. (13-16), where the input and output terms were interchanged such that the input is the mechanical force F_r from the ultrasonic transmitter, and the output is the electrical voltage V_o . This leads to:

$$\begin{bmatrix} F_r \\ u_r \end{bmatrix} = \begin{bmatrix} A_r & B_r \\ C_r & D_r \end{bmatrix} \begin{bmatrix} V_o \\ I_o \end{bmatrix} \quad (22)$$

where the transformation matrices are given as:

$$\begin{bmatrix} A_r & B_r \\ C_r & D_r \end{bmatrix} = \begin{bmatrix} A_0 & B_0 \\ C_0 & D_0 \end{bmatrix} \times \begin{bmatrix} A_2 & B_2 \\ C_2 & D_2 \end{bmatrix} \quad (23)$$

$$\begin{bmatrix} A_2 & B_2 \\ C_2 & D_2 \end{bmatrix} = \begin{bmatrix} e^{-\alpha h_m / 20} \cos \gamma_1 & e^{-\alpha h_m / 20} j Z_1 \sin \gamma_1 \\ (j \sin \gamma_1) / Z_1 & \cos \gamma_1 \end{bmatrix} \quad (24)$$

The matrix (A_0 , B_0 , C_0 , and D_0) is the same as that defined in Eq. (14). The transfer function relating the input sound force F_r to the receiver and the output voltage V_o converted by the receiver was determined as:

$$F_r = \frac{A_r Z_l + B_r + Z_l (C_r Z_{0t} + D_r)}{Z_l} V_o \quad (25)$$

where $Z_l = R_l + jX_{sl}$ is the electrical impedance of the voltage measuring instrument (e.g. an oscilloscope) connected to the ultrasound receiver outside the injection mold. Combining Eqs. (19) and (25), the relationship between the input voltage V_{tr} to the piezoelectric layer of the transmitter and the output voltage V_o delivered by the receiver was obtained as:

$$\frac{V_o}{V_{tr}} = \frac{Z_l Z_{0t}}{[A_r Z_{0t} + B_r + Z_s (C_r Z_{0t} + D_r)] [A_r Z_l + B_r + Z_l (C_r Z_{0t} + D_r)]} \quad (26)$$

Consequently, the energy efficiency of the ultrasonic transmitter across the steel mold is determined by:

$$\eta_{receiver} = \frac{P_{output}}{P_{input}} = \frac{V_o I_o}{F_r u_r} = \frac{Z_l}{[A_r Z_l + B_r + Z_l (C_r Z_{0t} + D_r)] [C_r Z_l + D_r]} \quad (27)$$

3.4. Model of the entire sensing system

Combining models of the various constituent components, the Bond graph model of the entire sensing system was obtained in Fig. 9. The top left part of the graph represents the energy converter with one TF element. The model illustrates the energy transformation from the melt pressure in the mechanical domain to the electrical charge in the electrical domain, then back to the mechanical domain via the ultrasonic transmitter, and ultimately back to the electrical domain through the injection mold, by way of the receiver. The total energy efficiency, involving the energy converter, the modulator, the transmitter, the injection mold, and the receiver, was obtained as:

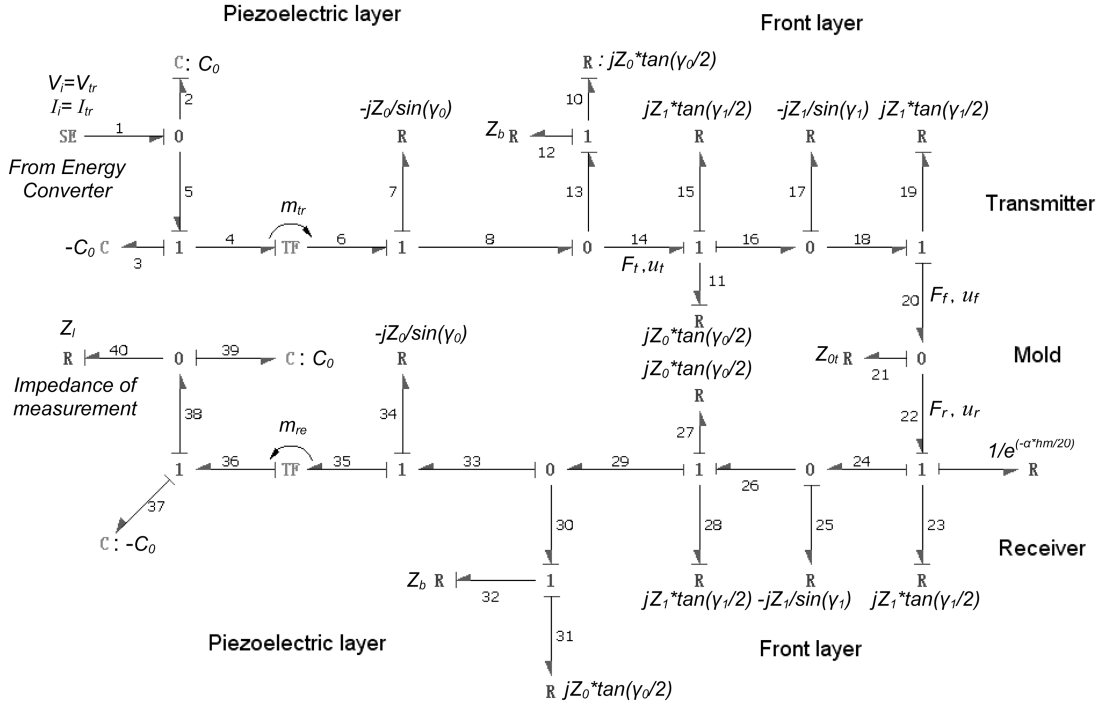


Fig. 9 Transmitter, injection mold and receiver Bond graph model

$$\eta = \eta_{converter} \times \eta_{transmitter} \times \eta_{receiver} \quad (28)$$

The developed Bond graph model was subsequently used as input to a commercial software package *SYMBOLS2000* in order to analyze the dynamic characteristics of the sensing system. Some of the parameters used for the analysis, including parameters for the piezoceramic stack in the energy converter, the ultrasonic transmitter, and the injection mold steel, are given in Tables 1 through 3, respectively.

4. Energy efficiency analysis

4.1. Energy efficiency of the converter

The efficiency of the energy converter model was evaluated as a function of the thickness of the piezoceramic rings as well as the charging time. A series of analysis were conducted, using 10 piezoceramic rings within the thickness range of 0.2-1 mm, and the charging time (pulsing cycle time) was varied between 1-5 ms. For a modulator pulsing cycle of 1 ms, the corresponding sensor resolution is 0.1 MPa, based an input ramp rate of the melt pressure of 100 MPa/second. Based on the Bond graph model analysis, the mechanical energy exerted by the melt was calculated to be 0.28 mJ, the transformer modulus $n_{tr}=12.7$ N/V, firing voltage $V_{tr} = 10.18$ V, and extracted electrical energy is 0.09 mJ. The corresponding energy efficiency η_r was found to be 32%. As shown in Fig. 10, the energy converter with a stack of 0.2 mm thick rings and 1 ms charging time has shown to

Table 1 Parameters of the piezoceramic stack in the energy converter (APC850 PZT)

Energy generator parameter	Symbol	Numerical value
Mass	m_{stack}	4.5 g
Damping	b_{stack}	150 Ns/m
Stiffness	K_{stack}	3×10^8 N/m
Piezoelectric ring thickness	h	0.001 m
Number of piezoelectric rings	n	10
Inner diameter of the ring	d_i	0.005 m
Outer diameter of the ring	d_o	0.01 m
Permittivity constant	e_{33}	1750
Charging constant	d_{33}	400×10^{-12} m/V
Young's modulus	Y	5.4×10^{10} N/m ²
Parallel capacitance	$C_{parallel}$	10.9 μ F
Stack capacitance	C_{stack}	9.12 pF

Table 2 Parameters of the piezoelectric transmitter and receiver

Transmitter Parameter	Symbol	Numerical value
Density of piezoelectric layer	ρ_t	7.7×10^3 kg/m ³
Density of front layer	ρ_f	8.0×10^3 kg/m ³
Electromechanical coupling factor	k	0.72
Longitudinal sound velocity	c_t	1220 m/second
Transmitter diameter	d	0.01 m
Permittivity constant	ϵ	1750
Thickness frequency constant	N_T	2032 m/second

Table 3 Parameters of the injection mold

Mold Parameter	Symbol	Numerical value
Density	ρ_m	7.85×10^3 kg/m ³
Electromechanical coupling factor	k	0.72
Longitudinal sound velocity	c_m	5850 m/second
Mold thickness	l_m	0.06 m

provide the maximum energy efficiency. This simulation confirms that using multiple thinner ring stack is better than using a single, thick ring, in terms of maximizing the energy efficiency of the converter.

4.2. Energy efficiency of the transmitter and the receiver

High energy efficiencies of the transmitter ($\eta_{transmitter}$) and receiver ($\eta_{receiver}$) allow for maximizing the energy conversions between the mechanical and electrical domains and consequently, maximizing the ultrasonic signal transmission power. To achieve such a design goal, the effect of the piezoelectric layer

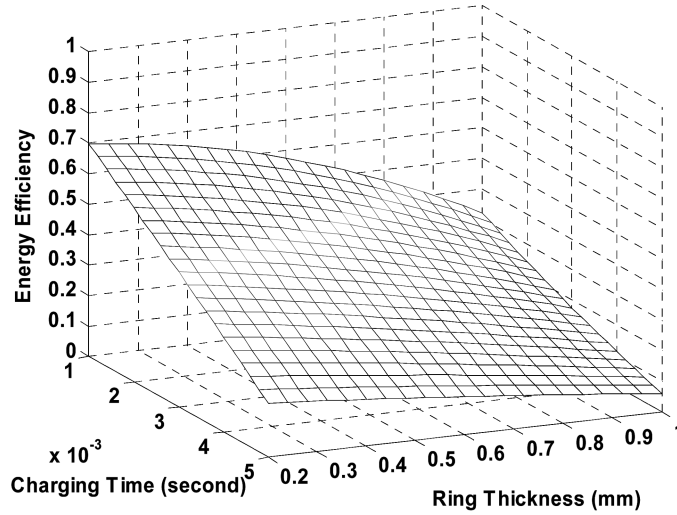


Fig. 10 Efficiency of the energy converter as a function of the piezoelectric ceramic ring thickness and charging time

and the front layers on the energy transfer in the sensing system was investigated, based on the Bond Graph model.

4.2.1. Selection of piezoelectric layer thickness

The effect of the piezoelectric layer on the energy efficiency of the transmitter-receiver sub-system was investigated by varying the thickness from 0.6 mm to 2.5 mm, with a step of 0.1 mm, assuming a front layer thickness of 1.2 mm. In Fig. 11, the corresponding energy efficiencies of the transmitter $\eta_{transmitter}$, the receiver $\eta_{receiver}$ and the combined energy efficiency $\eta_{transmitter} \times \eta_{receiver}$ are shown. The optimal piezoelectric layer thickness is defined as the thickness by which the product $\eta_{transmitter} \times \eta_{receiver}$ achieves the largest value. It is seen that the efficiency of the transmitter reaches its peak of 60.6% under a layer thickness of 1.0 mm, whereas the efficiency of the receiver reaches the maximum of 22.8% at 1.2 mm. Accordingly, the total energy efficiency of the system (the transceiver) reaches the maximum of 11.6%, at the piezoelectric layer thickness of 1.0 mm.

4.2.2. Selection of the front layer thickness

Based on the recommended optimal piezoelectric layer thickness of 1.0 mm, the effect of the front layer on the energy efficiency of the transmitter-receiver subsystem was subsequently investigated. This was done by varying the front layer thickness from 0.3 mm to 1.5 mm, at a step of 0.1 mm. Fig. 12 illustrates the energy efficiency of the transmitter, the receiver, and the combined transceiver system. It is seen that the efficiency of the transmitter reaches its maximum of 61.6% at the front layer thickness of 1.3 mm, whereas the efficiency of the receiver reaches the maximum value of 19.6% at the front layer thickness of 1.2 mm. Consequently, the total energy efficiency of the transceiver system reaches the maximum of 11.6% at the front layer thickness of 1.2 mm.

In addition to the thickness of the piezoelectric and front layers, simulation was also conducted to investigating the effect of the bonding layer on the energy efficiency. The result indicates that the effect is less than 0.5% relative to the total input energy. Consequently, the bonding layer thickness was considered negligible and not presented in the Bond graph model.

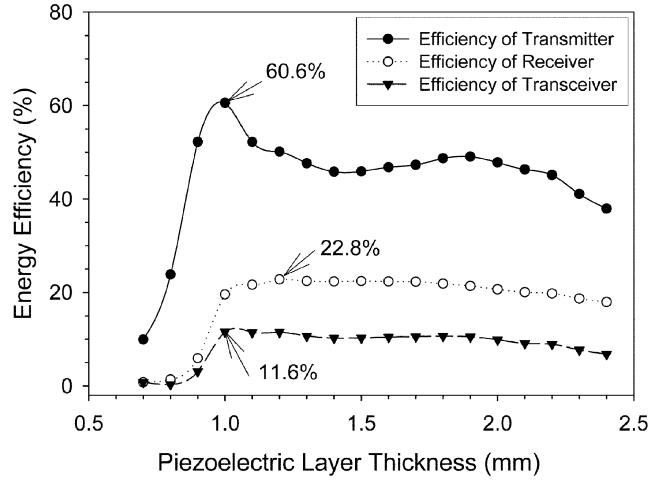


Fig. 11 Efficiencies of the signal transmitter and receiver as a function of piezoelectric layer thickness

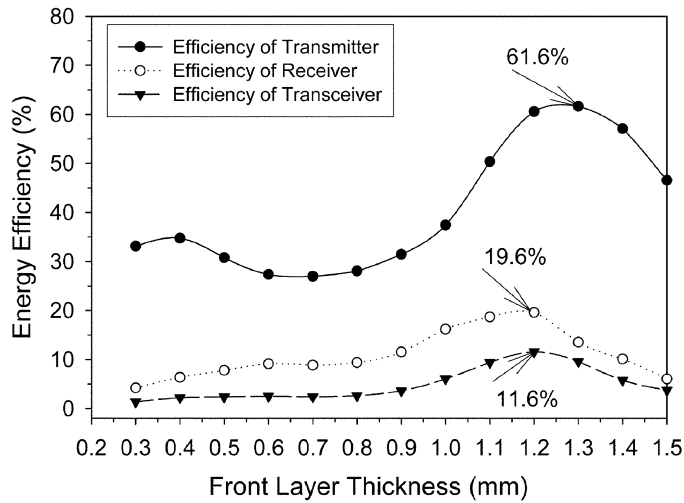


Fig. 12 Efficiency of the signal transmitter and the receiver as a function of the front layer thickness

5. Sensor design

The presented Bond graph model of the entire sensing system was used for assisting the sensor design. The primary decision variables included the frequency and power of the transmitted signal, as well as the geometric parameters of the energy converter and the ultrasonic transmitter. It was noted that multiple trade-offs needed to be resolved in the sensor design. The most significant issue was that a higher power signal will require a geometrically larger energy converter or, alternatively, fewer pulses to be transmitted, given the energy availability. A reduction in the number of pulses corresponds to an increase in the pressure change per pulse and thus a decrease in the sensor resolution. The Bond graph model was used to resolve these issues according to the methodology provided in Fig. 13, which is the inverse of the analysis process illustrated in Fig. 3.

the ultrasonic transmitter. Consequently, the electrical energy that was required to generate this signal was found to be $W_{elec} = 0.09$ mJ. Given the frequency and energy requirements, the Bond graph model was further used to design the transmitter. The analysis shown above indicates that the combination of 1.0 mm and 1.2 mm presents the optimal thickness for the piezoelectric layer and front layer, respectively. When excited, a transmitter with these layer thickness values will generate ultrasonic pulses with a relatively large energy efficiency 11.6%.

The Bond graph model was then used to analyze the energy conversion and design the energy converter. To generate W_{elec} of 0.09 mJ, the Bond graph model was iteratively executed to evaluate the efficiency and design parameters of the energy converter. In general, a small diameter is preferred with a length-to-diameter ratio between 2 and 3. Accordingly, the final design was found to be 10 mm in diameter, 20 mm in length, with an energy conversion efficiency of 32%. Consequently the total energy efficiency for the entire sensing system was found to be $32\% \times 11.6\% = 3.8\%$.

Given a typical injection molding process with a dynamic pressure of 100 MPa/sec, the designed sensor will have a minimum sensitivity of 0.1 MPa, which corresponds to a 0.5% accuracy relative to a conventional sensor with a 200 MPa full-scale output. The minimum response time was found to be 1 ms, which is an order of magnitude below the 1 ms sweep time currently used in molding process controllers. As indicated by the outer loop in Fig. 13, the Bond graph model can be used to trade-off sensor size, resolution, and response time for various receivers and application requirements. Such integrated systems analysis has facilitated the rapid and accurate estimation of the design's performance, thereby increasing the quality of the design and reducing development risk.

6. Experimental evaluation

The result of the Bond graph model-based energy analysis was verified by two experimental case studies. The first study was designed to verify the energy efficiency of the energy converter, whereas the second study was focused on testing whether ultrasound pulsing can be detected by the receiver within the given energy range.

6.1. Evaluation of energy converter efficiency

A ramp force input was used as the input to mechanical port of the energy converter. The input force lasted about 1.5 ms and the maximum pressure on the piezoceramic stack was measured to be approximately 0.1 MPa. Such values closely resembled the condition within the mold cavity during an injection molding process. The prototype energy converter was built using a stack of the APC850 piezoceramic rings, with the same configuration as shown in Table 1. The input force was measured by a PCB-201B03 force sensor mounted in series with the piezoceramic stack. The output voltage of the stack was measured and recorded by a Tektronix TDS3012B digital oscilloscope. The input mechanical energy and output electrical energy were calculated based on these data shown in Table 1. In Fig. 14, the input mechanical energy and output electrical energy from both the experimental stack and the Bond graph model are illustrated. It is seen that the predicted output energy output curve based on the Bond graph model closely followed the experimental output energy curve, and the corresponding energy efficiency values were found to be 25.5% and 26.1%, respectively.

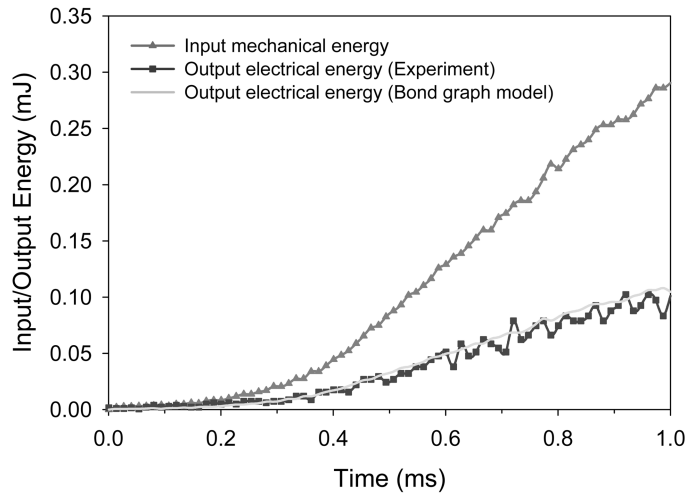


Fig. 14 Mechanical and electrical energy applied to and extracted from the energy converter during a pulsing cycle: simulation and experiment

6.2. Evaluation of transmitter and receiver models

To verify the Bond graph model of the ultrasonic transmitter, a piezoceramic disk (PKI501) of 1 mm thickness and 2.21 MHz resonant frequency was utilized as the piezoelectric layer of the transmitter. The thickness was chosen to be as the optimal layer thickness recommended by the Bond graph model. In addition, two discs of 1.7 mm and 0.85 mm thick and 2.8 MHz and 1.5 MHz resonant frequencies, respectively, were chosen to represent non-optimal layer thickness. The thickness of the front layer was chosen to be 1.2 mm for the three transmitters. The input electrical impedance was 50Ω , measured using an impedance analyzer (HP 8753C). A Pulser (model PAC C-101-HV) was used to generate electrical pulses simulating the threshold modulator. Given the input voltage of 10 V, the corresponding input electrical energy was calculated to be 0.09 mJ. The transmitter was coupled to a steel block of 60 mm thickness, through a $60 \mu\text{m}$ coupling layer of grease. The signal transmitter excited by the electrical pulse generated ultrasonic pulses, which were then transmitted through the mold steel to a signal receiver (GE Panametrics A180R). In Fig. 15, a comparison of the simulated and experimentally measured ultrasonic pulses generated by the transmitter under three different piezoelectric layer thicknesses is shown.

It is seen that the measured ultrasonic pulses are generally in very good agreement with the simulated pulses predicted by the Bond graph. Given the SNR of the receiver is 20 dB and the measurement noise level is about 1 mV, the corresponding minimum receiver output is 10 mV. Consistent with the Bond graph prediction, the output from the optimal transmitter (with 1.0 mm piezoelectric layer thickness) has shown in both the time and frequency domains the best matching between the simulation and the experimental results, as illustrated in the bottom portion of Fig. 15. The measured peak values of the ultrasonic pulse are around 15 mV (time domain) and 10 mW (frequency domain), which are about 3 to 5 times as large as the peak values from the other two transmitters, respectively. This indicates a high energy efficiency of the transmitter design, which ensures that pulse trains transmitted by the ultrasonic transmitter can be reliably detected by the receiver, and the discretized pressure information can be extracted from the noise.

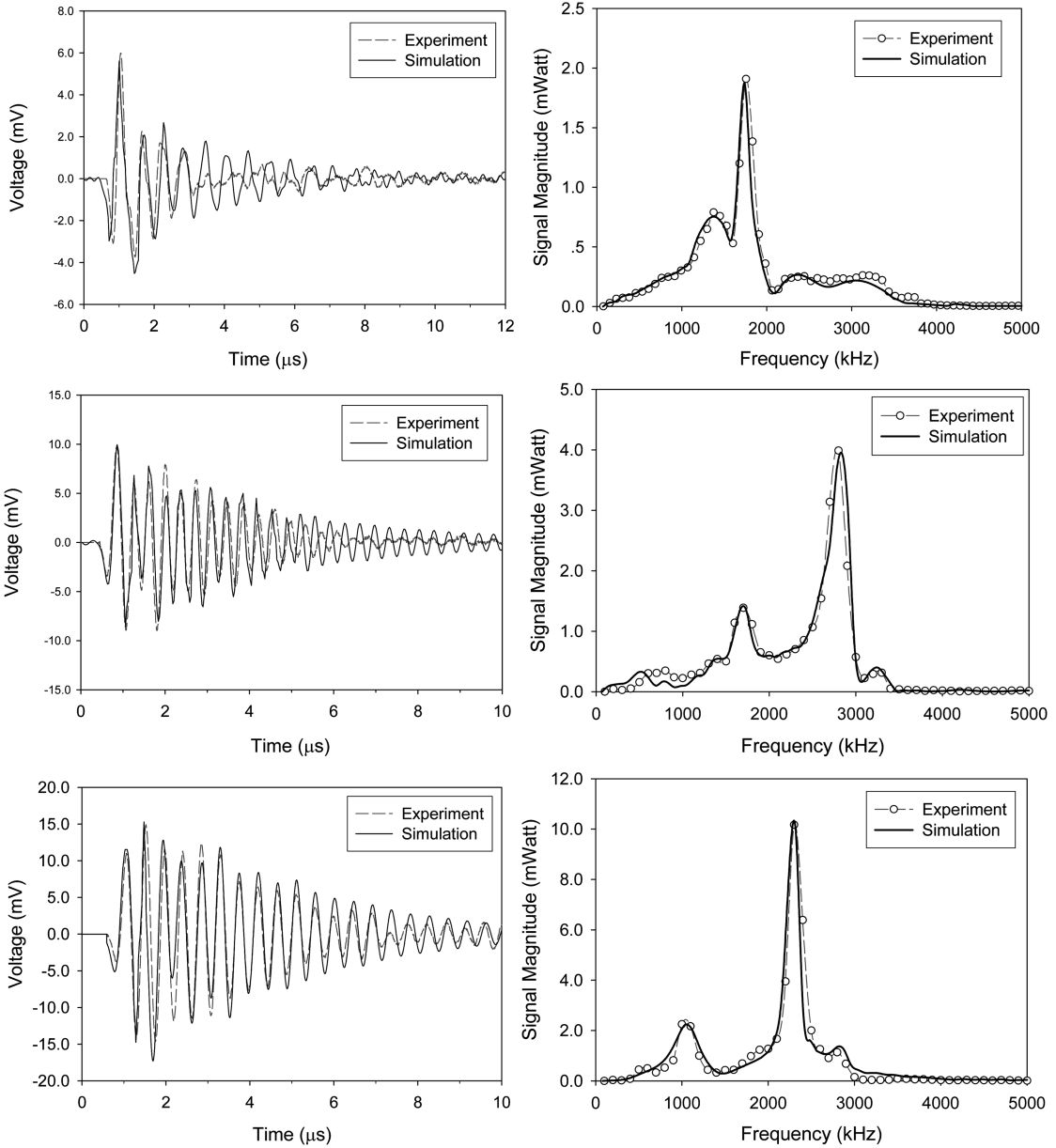


Fig. 15 Measured and simulated ultrasonic pulses from the transmitter under three different piezoelectric layer thicknesses: (top) 1.7 mm, (middle) 0.85 mm, and (bottom) 1.0 mm

7. Conclusions

Bond graph modeling has shown to be an effective tool in both analyzing an embedded pressure sensor system involving energy transfers between different domains and guiding the design and parameter optimization of the sensor configuration. Given the linear nature of the constituent components involved in the sensor system, the modeling process was readily completed using causal frequency-

domain models. The Bond graph models developed in this study indicate that the energy efficiency of the mold-embedded pressure sensor is predominantly affected by the configuration of the piezoceramic stack and the thicknesses of the various layers in the transmitter. Analysis and experiments have shown that a stack with multiple thin (0.2 mm) rings can extract more electrical energy than a stack with less but thicker rings, under the same total stack height and mechanical energy input. Similarly, under the same electrical energy input, a transmitter with 1.0 mm piezoelectric layer and 1.2 mm front layer generates ultrasonic pulse trains of the highest magnitude. Based on the good agreement found between the experiments and the simulations, it is noted that Bond graph, although having been developed several decades ago, continues to provide a viable and efficient tool in complex system modeling and design optimization. Its utilities should be fully explored for the design of a new generation of sensors and smart structures and components that enable such capabilities as compact size, high energy efficiency, self-powering, and self-diagnosis, to meet the increasing demands of both the industry and consumers.

Acknowledgements

The authors gratefully acknowledge funding provided to this research by the National Science Foundation under awards DMI-9988757 and DMI-0428366.

References

- Bray, D. E. and McBride, D. (1992), *Nondestructive Testing Techniques*, John Wiley & Sons, Inc., New York.
- Busch-Vishniac, I. J., and Paynter, H. M. (1991), "Bond graph models of acoustical transducers", *J. Franklin Inst.*, **328**(5-6), 663-673.
- Gao, R., Kazmer, D., Zhang, L. and Theurer, C. (2002), "Design of a self-energized sensor for injection molding process monitoring", *Proceedings of the NSF Design, Service and Manufacturing Grantees and Research Conference*, San Juan, Puerto Rico, January 7-10.
- Goldfarb, M., and Jones, L. D. (1999), "On the efficiency of electric power generation with piezoelectric ceramic", *J. Dyn. Syst., Measurement, Control*, ASME, **121**, 566-571.
- Goldfarb, M. and Celanovic, N. (1997), "A lumped parameter electromechanical model for describing the nonlinear behavior of piezoelectric actuators", *J. Dyn. Syst., Measurement, Control*, ASME, **119**(3), 478-485.
- Karnopp, D. and Rosenberg, R. (1968), *Analysis and Simulation of Multiport Systems: The Bond Graph Approach to Physical System Dynamics*, The M.I.T. Press, Cambridge.
- Karnopp, D. Margolis, D. and Rosenberg, R. (2000), *Systems Dynamics, Modeling and Simulation of Mechatronic Systems*, John Wiley & Sons, Inc. New York.
- Margolis, D. and Shim, T. (2001), "A bond graph model incorporating sensors, actuators, and vehicle dynamics for developing controllers for vehicle safety", *J. Franklin Inst.*, **338**(1), 21-34.
- McBride, R. and Cellier, F. (2003), "Object-oriented bond graph modeling of a gyroscopically stabilized camera platform", *Proceedings of the International Conference on Bond Graph Modeling and Simulation, ICBGM'03 Conference*, Orlando, FL.
- Montgomery, R. and Granda, J. (2003), "Using bond graph for articulated, flexible multi-bodies, sensors, actuators and controllers with application to the international space station", *West MultiConference on Computer Simulation*, 2003, Orlando, FL.
- Rawabdeh, I. A. and Petersen, P. F. (1999), "In-line monitoring of injection molding operations: A literature review", *J. Injection Molding Technology*, **3**(2), 47-53.
- Sakurai, Y. (2000), "Calculation of dynamic overall efficiency of a load sensing hydraulic system by bondgraphs",

- Industrial Electronics Society, 2000. IECON 2000. 26th Annual Conference of the IEEE, Nagoya, Japan.*
- Sittig, E. K. (1969), "Effects of bonding and electrode layers on the transmission parameters of piezoelectric transducers used in ultrasonic digital delay lines", *IEEE Trnascrions on Sonics and Ultrasonics*, **SU-16**, 2-10.
- Theurer, C., Zhang, L., Kazmer, D. and Gao, R. (2003), "In-situ evaluation of a piezoelectric energy extraction device for wireless cavity pressure sensing in injection molding", *Proceedings of the 2003 ASME International Mechanical Engineering Congress & Exposition, Dynamic Systems & Control Division*, Washington, D. C.
- Waanders, J. W. (1991), *Piezoelectric Ceramics Properties and Applications*, Philips Components, Eindhoven.
- Watkins, B. H. (1997), "Five myths about sensing mold pressure", *Sensors Magazine*, **14**, 73-78.
- Youcef-Toumi, K. (1996), "Modeling, design, and control integration: a necessary step in mechatronics", *IEEE/ASME Transactions on Machatronics*, **1**(1), 29-38.
- Zhang, L., Theurer, C., Gao, R. and Kazmer, D. (2003), "Frequency design of an ultrasonic transmitter for injection molding pressure measurement", *Transactions of the North American Manufacturing Research Institute of the Society of Manufacturing Engineers*, **31**, 579-586.
- Zhang, L., Theurer, C., Gao, R. and Kazmer, D. (2005), "Design of ultrasonic transmitters with defined frequency characteristics for wireless pressure sensing in injection molding", *IEEE Transactions on Ultrasonics, Ferroelectrics, and Frequency*, **52**(8), 1360-1371.

Appendix A

To derive the expression for the transformer modulus n_{tr} , it is noted that the pressure generated by the melt on the piezoceramic stack is $P = F/A$. Under this pressure, each piezoceramic ring will experience a displacement of x , which equals to $F \cdot h / A \cdot Y$, with Y being the Young's modules of the piezoceramic material, and h being the thickness of the piezoceramic ring. As illustrated in Fig. 5, the energy transferred from the mechanical domain to the electrical domain can be expressed as $F_{tr} \cdot x$. According to the energy conservation law, the voltage developed across the piezoceramic ends is represented by $F_{tr} \cdot x = V_{tr} \cdot q$ and $V_{tr} = F_{tr} / n_{tr}$, with q being the electrical charge. The charge density resulting from the piezoelectric effect can be determined (Waanders 1991) by:

$$\frac{q}{A} = n d_{33} \frac{F}{A} \quad (\text{A-1})$$

where d_{33} is the piezoelectric charge constant and n is the number of piezoelectric rings in a stack. The following equation can then be obtained:

$$F_{tr} \frac{Fh}{AY} = \frac{F_{tr}}{n_{tr}} n d_{33} F \quad (\text{A-2})$$

Finally, the expression of n_{tr} can be obtained as:

$$n_{tr} = \frac{n A d_{33} Y}{h} \quad (\text{A-3})$$

Given the piezoceramic stack with parameters as shown in Table 1, the transformer ratio was found to be $n_{tr} = 12.7 \text{ N/V}$.

Appendix B

The transfer function of the energy converter is determined by the input force (F) from the polymer melt and the output voltage (V_{tr}). Based on the Bond graph model shown in Fig. 5, the state space formulation can be derived as:

$$\begin{bmatrix} \dot{q}_4 \\ \dot{p}_6 \\ \dot{q}_8 \end{bmatrix} = \begin{bmatrix} 0 & \frac{1}{I_6} & 0 \\ -\frac{1}{C_4} & \frac{R_3}{I_6} & -\frac{n_{tr}}{C_8} \\ 0 & \frac{n_{tr}}{I_6} & -\frac{1}{C_8 R_9} \end{bmatrix} \begin{bmatrix} q_4 \\ p_6 \\ q_8 \end{bmatrix} + \begin{bmatrix} 0 \\ 1 \\ 0 \end{bmatrix} E_1 \quad (\text{B-1})$$

where q_4 , p_6 and q_8 are the state variables. Based on the expressions of intermediate parameters $I_6 = m_{stack}$, $E_1 = PA$, $C_4 = 1/k_{stack}$, $R_3 = b_{stack}$, $q_4 = x_{stack}$, $F_{tr} = q_8 \cdot n_{tr}/C_8$ and $p_6 = m_{stack} \dot{x}_{stack}$, the dynamics of the energy converter is found to be:

$$m_{stack} \ddot{x}_{stack} + b_{stack} \dot{x}_{stack} + k_{stack} x_{stack} + F_{tr} = PA \quad (\text{B-2})$$

where the melt pressure $P(t) = P_{max} \cdot t/t_p$, with P_{max} being the maximum pressure, and t_p is the stack charging time. The surface area of the sensor cap is given by $A = \pi d_o^2/4$. The symbol d_o denotes the outer diameter of the piezoceramic stack.

From the electrical portion of the Bond graph model, it is seen that $C_8 = C_{stack} + C_{parallel}$, $q_8 = q$ and $e_8 = V_{tr}$, from which the following relationship can be established:

$$q = (C_{stack} + C_{parallel})V_{tr} \quad (\text{B-3})$$

where the capacity of the stack C_{stack} is calculated by:

$$C_{stack} = ne_{33}e_r \frac{\pi(d_o^2 - d_i^2)}{4h} \quad (\text{B-4})$$

with e_{33} being the permittivity constant, and $e_r = 8.85 \times 10^{-12}$ F/m is the permittivity of the free space. The symbol d_i denotes the inner diameter of the ring.

From Eqs. (2), (3), (B-2) and (B-3), the transfer function of the energy converter is found to be:

$$\frac{V_{tr}(s)}{P(s)} = \frac{An_{tr}}{(C_{stack} + C_{parallel})(m_{stack}s^2 + b_{stack}s + k_{stack}) + n_{tr}^2} \quad (\text{B-5})$$

The transfer function provides for the dynamic relationship between the output voltage V_{tr} from the energy converter and the input melt pressure P . From Eqs. (3) and (B-3), the displacement of the stack can be calculated as $x_{stack} = (C_{stack} + C_{parallel})V_{tr}/n_{tr}$.